Will mixing rule or chemical reactions dominate the ash behavior of biomass mixtures in combustion processes on laboratory and pilot scales?

Emile Atallah, Françoise Defoort, Matthieu Campargue, Capucine Dupont, Alexander Pisch

Will mixing rule or chemical reactions dominate the ash behavior of biomass mixtures in combustion processes on laboratory and pilot scales?

Emile ATALLAH[1], Françoise DEFOORT[1], Matthieu CAMPARGUE[2], Alexander PISCH[3], Capucine DUPONT[4]

[1] Université Grenoble Alpes, Commissariat à l'Energie Atomique et aux Energies Alternatives (CEA), Laboratoire d'Innovation pour les Technologies des Energies nouvelles et les Nanomatériaux (LITEN), DTCH, F-38000 Grenoble, France
[2] RAGT Energie, F-81000 Albi, France
[3] Université Grenoble Alpes, CNRS, Grenoble INP, SIMaP, 38000 Grenoble, France
[4] IHE Delft Institute for Water Education, Department of Water Supply Sanitation and Environmental Engineering, Delft, the Netherlands

Abstract

Mixing biomasses has a good potential to solve operational problems in thermochemical valorization processes related to ash behavior. Chemical reactions within the ash of the blend, and not only a mixing effect without reaction, need to take place to form new solid phases in the mixture at the expense of getting rid of the problematic liquid one to decrease the slagging tendency. The present work focuses on assessing the presence of a chemical reaction in comparison with a simple mixing effect within the ash of mixtures of wheat straw - oak bark biomass and ash in two laboratory setups and in a fixed and in a moving bed pilot combustion reactors. The operating conditions were varied to study their effects on the reactivity of the ash within the mixtures. This aimed to optimize the ash reactivity and to assess the capabilities of the laboratory test to predict the ash behavior in pilot-scale reactors.

Mixing without reaction effect was more evident when mixtures of biomass were used on both laboratory and pilot scales. In this case, the simple mixing rule was able to simulate the general ash behavior of biomass mixture to a certain extent that exact prediction was always limited by the presence of certain chemical reactions. However, chemical reactions effect was dominant when mixtures of ash of biomass were applied as feedstock. Solid crystalline phases $K_2Ca_2Si_2O_7$ and $K_2Ca_6Si_4O_{15}$ were the direct end products of these chemical reactions. Their relative proportion was inversely proportional to the problematic amorphous phase in the final ash. Hence, optimizing the blend proportion to increase their concentrations has the potential to solve slagging problematic. These two compounds were mostly stable at 1000°C, at which equilibrium was reached after 6h. However, they existed at a lower proportion at 850°C and disappeared at 1200°C. The developed laboratory pellet test was also able to predict very efficiently the pilot ash behavior of both individual biomasses and their mixture in terms of crystalline and amorphous composition and proportion along with agglomeration distribution.

Keywords: Biomass mixing, biomass ash, prediction approach, pilot plant scale, chemical reaction, operating conditions.

1. Introduction

The worldwide energy demand is continuously increasing with the population and economic growth, and is projected to reach around 250000 TWh in 2040 [1]. Biomass, when used as fuel in thermal conversion processes such as combustion or gasification, has the potential to satisfy more than 60% of this increasing energy demand [2]. However, these fuels are characterized by various ash yields [3,4] and a wide range of ash compositions that induces various problems when applied in thermochemical conversion processes [5].

Many agricultural residues, such as wheat straw, are characterized by high alkali-silicate contents that lower the melting point of the resulting ash and lead to the occurrence of a liquid phase, even at relatively low temperatures (i.e. 800°C) [6]. Hence, they can form agglomerates in fluidized bed reactor (FBR), i.e. ash in the liquid phase that sticks or reacts with the bed materials, or induce sintering effects in furnaces, i.e. ash in the liquid phase that sticks to the bottom of the reactor or its walls. This can lead to blocking, fouling, clogging the reactor along with instrument shutdown, poor degradation by combustion reaction, and increased operational costs [7]; ash in the solid phase is preferred in this case. On the contrary to the cases of the furnace and the fluidized bed, ash in the liquid phase is highly needed in an entrained flow reactor (EFR) to control the temperature and flow of ash on the walls [8,9].

In contrast with agricultural residues, ash of wooden biomass is rich in calcium-silicates that produce ash in the solid phase, even at high temperatures (i.e. 1300°C), which makes them good candidates for furnace and FBR but not for EFR. Consequently, using one type of biomass can yield ash in either the solid or the liquid phases, or even sometimes produce a mixture of liquid-solid phases; hence posing several limitations on the applied process.

Additives were widely used to decrease agglomeration and sintering levels, but each has its own problem [10–13]. Their cost is usually high and their application depends on the

feedstock [10,14]. Aluminosilicates based additives were able to effectively reduce the fine particulate matter emissions, but they increased the gaseous emissions of HCl and SO_x [15]. Kaolin also proved to be a good additive especially in decreasing the slag formation; but they tend to increase HCl, SO_x, and NO_x emissions [10,16]. This was the similar case with dolomite additives [17]. Phosphorous based additives, such as $NH_4H_2PO_4$ in the work of Wang et al. [18], successfully decreased slag formation, but at the same decreased the integrated combustion characteristic index and their efficiency depended on the inorganic composition of the fuel that they were added to. On the other hand, biomass mixing proved to be a more suitable solution than additives to fight slagging and agglomeration in terms of cost and effectiveness [19] and triggered the interest of many researchers during the last thirty years [6,20–24]. Mixing biomasses with different ash contents and compositions at various ratios modifies the chemical composition and physical properties of the feedstock. Then upon heating, chemical reactions within the ash can take place to form new solid phases in the mixture and reduces therefore the percentage of the liquid phase [2-3]. However, mixing without interaction can also take place, hindering the chemical reactions and enhancing the problematic phase. The chemical reactions within the ash of the biomass mixture, which highly depend on operating conditions, were the interest of several researchers in the field [6,21,25–27], especially in laboratory-scale experiments. Some of them suggested various reaction pathways that might take place between the inorganic elements of the ash of biomass [6,28,29].

Biomass mixing can affect ash behavior not only in laboratory furnaces but also in pilot reactors. For instance, Salour et al. [30] cofired wood and straw in a more than 50% wood fraction mixture in a pilot fluidized bed combustor at 800°C. They have found that bed agglomeration was intensified when straw reached 50 wt.% in the wood-straw mixture due to an increasing interaction within the ash of the two biomasses as straw fraction increased in the

50 blend [30]. Nordgren et al. [31] co-fired wheat straw and softwood bark in a 150 kW pulverized
51 fuel-fired burner and found that the tendency for both fouling and slagging was reduced when
52 mixtures were applied instead of single biomasses. They referred to both a dilution (i.e. mixing
53 without chemical interaction) and interaction effect taking place in the straw-bark mixtures
54 [31]. In their study, Zeng et al. [21] used various binary mixtures of wood, wheat straw, and
55 miscanthus in a small scale combustion appliance with a nominal heat capacity of 30 kW. They
56 found that adding wood to straw significantly increased the bed and sintering temperatures,
57 especially in the mixtures with more than 70 wt.% wood [21].

58 Instead of trial-and-error or systematic proportional mixing from 0 to 100, a prediction tool can
59 be developed to adapt the type and composition of the biomass mixture to the applied process.
60 Empirically derived indices are widely used to predict the ash behavior of coal but showed
61 significant limitations in the case of biomass [24,32–34]. This might be due to the abundant
62 iron and alumina-silicate ash contents in coal compared to the high calcium and alkali-silicates
63 in biomass [24,32]. Several researchers proposed the use of a thermodynamic tool, i.e. the CaO-
64 K_2O-SiO_2 ternary phase diagram to predict ash behavior, such as Rebbling et al. [28], Zeng et
65 al. [21], Defoort et al. [27], and Ohman et al. [7]. Despite the relative success of such a
66 prediction tool, the same authors concluded that the thermodynamic database needs to be
67 revised since some crystalline phases appeared experimentally but were absent in the database
68 [27], and the calculated liquidus line differed from the experimental results [21,28]. The main
69 drawback of the thermodynamic prediction tool is that it provides results at equilibrium, which
70 might or might not be the case in real processes, especially on an industrial scale. Hence,
71 laboratory tests are still a mandatory step to evaluate the ash behavior in a pilot plant.

72 Various laboratory ash behavior prediction tests were used to investigate the behavior of
73 biomass mixtures, such as the Bioslag test [24], thermogravimetric analysis-differential thermal
74 analysis (TGA-DTA) [35], rapid qualitative test [36], and standard ashing test [35]. However,

these tests are usually time-consuming, were rarely compared to results obtained on a pilot scale, and depend on the feedstock, reactor type, and operating conditions [24,35]. For instance, Gilbe et al. [37] compared the slagging tendencies predicted by the ash fusion test (SS ISO-540), TGA/DTA, thermodynamic phase diagrams, and a laboratory scale-sintering test with those in a 20kW pilot reactor. They used 12 different single biomasses, including wheat straw and various barks, and they found that the four laboratory tests failed to quantitatively predict the slagging behavior in the pilot, leading to different experimental results when compared with the predicted values [37]. However, these methods were able to predict the same fuel-specific slagging qualitative trends as the corresponding combustion behavior [37]. Authors mentioned that further improvements need to be done on the tests, especially the TGA/DTA and the SS ISO 540 tests [37].

In this work, single bark, single straw and their 50-50 mixture in the form of biomass and ash were used in two different laboratory combustion set-ups and in fixed and moving bed combustion pilot reactors. This work applied full crystalline phase quantification (including the amorphous phase), instead of the limited semi-quantification in the previous work of Defoort et al. [27] for example. The first and main objective was to evaluate the presence of chemical reactions in contrast with mixing without interaction within the ash of the mixtures. The second objective was to study the effect of temperature, residence time, and cooling rate on the ash reactivity of the mixtures on laboratory scale. This helped find the optimum equilibrium condition at which the ash problematics were at minimum, in the case of straw-bark mixture. In addition, by comparing the experimental results of the laboratory tests under the various operating conditions against those in the pilot scale combustion reactors, the capabilities of the laboratory tests to predict the ash behavior of biomass mixtures in pilot reactors were assessed. To our knowledge, this type of assessment was never done, especially using biomass mixtures, in any of the aforementioned laboratory prediction tests.

2. Materials and methods

2.1. Feedstock

Defoort et al. [27] found that 50-50 wt.% biomass bark-straw mixture (called MP2b) lies in the middle of the solid section in the ternary phase diagram $CaO-K_2O-SiO_2$, and hence it will be applied in this work. The elemental composition of every single biomass, i.e. oak bark, wheat straw, and their 50-50 wt.% biomass bark-straw mixture (i.e. MP2b), was measured by an Elementar Vario EL cube CHNS Analyzer along with an inductively coupled plasma atomic emission spectroscopy (ICP−AES) and were the same as the ones presented in related previous work [27]. The measured elemental composition of the biomasses and their mixture is shown in Table 1.

Bark weight fraction in the ash bark-straw mixture (β) can be calculated from bark weight fraction in the biomass bark-straw mixture (α), taking into account the ash yield of the parent fuels (noted A_1 for bark and A_2 for straw) and is:

$$\beta = \alpha A_1/(\alpha A_1 + (1-\alpha)A_2) \quad (1)$$

Then a mixture of 50% biomass bark corresponds to 61% ash bark in wheat straw biomass or ash respectively.

Table 1: Measured elemental composition and ash weight percentage of each biomass feedstock.

			straw	**bark**	**MP2b**
	Norm	**Relative uncertainty**	*wt.%*		
C	NF EN 15104	±1%	43.60	48.60	46.10
H	NF EN 15104	±2%	5.50	5.80	5.65
O	By difference		47.27	41.37	44.29
N	NF EN 15104	±15%	0.54	0.60	0.57
Ca	NF EN ISO 16967	±5%	0.29	2.56	1.43
K	NF EN ISO 16967	±5%	1.43	0.26	0.85
Si	ICP internal method	±5%	0.99	0.48	0.74
S	EN 15289	±15%	0.09	0.04	0.07
Cl	EN 15289	±15%	0.14	0.01	0.07

P	NF EN ISO 16967	±5%	0.07	0.03	0.05
Al	NF EN ISO 16967	±5%	0.00	0.07	0.04
Mg	NF EN ISO 16967	±5%	0.05	0.07	0.06
Fe	NF EN ISO 16967	±5%	0.01	0.03	0.02
Na	NF EN ISO 16967	±5%	0.02	0.01	0.02
Mn	NF EN 15297	±10%	0.00	0.07	0.04
Ash 550°C	NF EN 14775	±5%	6.3	9.7	6.7

2.2. Experimental setup

Three types of tests were applied. The first two tests (ash test (A) and pellet test (P)) were already described in the work of Defoort et al. [27] and are reminded below:

1. Ash test (A) in which biomass pellets (1.5cm x 0.5cm) were heated at 550°C for 2h in static atmospheric conditions in a Nabertherm LT 15/11/330 furnace then cooled down to room temperature. This step at 550°C helped to get rid of all organic oxygen and hydrogen (along with organic nitrogen and part of chlorine) while preserving the majority of the other elements. Afterwards 0.5 g of ash were compressed as ash chips (1.3 cm diameter) under a pressure of 10 bar to favor the contact between the inorganic particles. The compressed ash chip was put in a 95-5 wt.% Pt-Au crucible – this material was selected to avoid any interaction between the sample and the crucible - and was heated in a vertical Nabertherm RT 50-250/13 furnace in static atmospheric conditions at a heating rate of 10°Cmin until the setpoint temperature was reached. Residence time in Table 2 started to be counted when the final temperature was reached. At the end of each experiment, samples were quenched in the air [i.e. ~5°C /s] until room temperature. These laboratory conditions favor chemical equilibrium (strong proximity of ash grains).
2. Pellet test (P) where biomass pellets (1.5cm x 0.5cm) were heated directly in a Nabertherm LT 15/11/330 furnace in static atmospheric conditions at a heating rate of 10°C/min until the setpoint temperature was reached. Residence time started to be counted when the

setpoint temperature was reached. At the end of each experiment, samples were quenched in the air [i.e. ~5°C /s] until room temperature. These laboratory conditions simulate the conditions in a pilot reactor (low proximity of ash grains dispersed in the biomass matrix).

3. Pilot test (Pilot) where biomass pellets (1.5cm x 0.5cm) were burned. 10 kg/h of the biomass pellets were combusted in a 30 kW Guntamatic Powercom moving bed boiler for 5h. In addition, 5 kg/h of biomass pellets were combusted in a 25 kW Multiheat 2.5 fixed bed furnace for 2h. Three thermocouples were inserted in the furnace of the fixed bed reactor to measure the temperature during the test. The same compressed biomass pellets of the 50:50 mixture (MP2b) that were used in the pellet test were applied in the two pilot reactors. However, individual straw and bark biomass pellets were used in just the fixed bed boiler.

Temperature and residence time varied in each laboratory test as indicated in Table 2. Cooling rate (slow cooling [i.e. ~0.05°C/s] versus quenched cooling [i.e. ~5°C/s]) was varied for just the ash test at 1000°C and 6h, while quenching was applied in all the other experiments. Each test was performed in duplicate. The oven for the pellet test was not able to reach 1200°C (maximum operating temperature of 1000°C).

An external k-type thermocouple was introduced in the Nabertherm LT 15/11/330 used in the pellet test and the Nabertherm RT 50-250/13 used in the ash test. It was found that the measured temperature in both furnaces in early residence times was different from the final set point temperature by ± 20°C. Hence, ash and pellet test experiments at 20 minutes residence were slightly more inaccurate in terms of operating temperature. However, due to the high-applied temperature range and the small temperature deviation, the results were still considered as being acceptable.

Table 2: Temperature and residence time combination in the ash (A) and pellet (P) tests.

	20min	1h	2h	3h	4h	5h	6h	24h	40h
850°C	P	P					A	A	
1000°C	A & P	A & P		A	A	A	A & P		A
1200°C	A	A	A	A			A		

2.3. Analysis instruments and methods

2.3.1. P-XRD analysis

Bruker D8 Advance Powder X-Ray diffraction (P-XRD) with Cu Kα (40 kV and 30 mA) was used to analyze qualitatively and quantitatively the various solid phases present in the samples along with the amorphous content. Samples were manually ground by a mortar and placed in an amorphous silica sample holder then flattened with glass to obtain a well-defined surface. Diffractograms were obtained over a 2θ interval between 15° and 70°. Identification along with semi-quantification of the crystalline phases was first performed using Bruker EVA software along with its I/Icor module. The Diffractograms of all the samples are shown in the appendix. However, instead of the simple semi-quantification using I/I_{cor} modulus in EVA software as proposed in the work of Defoort et al. [27], full XRD quantification was conducted by applying Rietveld refinement to each sample using Panalytical Instruments Highscore plus software after adding 10 wt.% of TiO2 Anatase (99.99 wt.%, Sigma-Aldrich) as an internal standard to quantify the amorphous phase (assumed to be solidified liquid silica-rich phase). Taking into consideration the high operating temperature of 850°C, 1000°C, and 1200°C, the majority of the organic materials (chars) should have decomposed and volatilized into the gaseous phase. Hence, their concentration was assumed to be negligible in the amorphous phase in this work. ICDD 2020 crystallography database was used in the two aforementioned software.

For the quantification of the amorphous phase, 10 wt.% of TiO_2 Anatase powder was crushed, manually ground, and mixed with the sample in a way to fill the sample holder (~0.25g total mass of sample and TiO_2 standard in each analysis). Hence, the Rietveld analysis for the diffractogram of the XRD of each sample gave the weight percentage of all the crystalline phases in the presence of TiO_2 Anatase (standard). To get the amorphous percentage and the real percentage of the other crystalline phases (i.e. in the pure sample without Anatase), the real total weight of the pure sample (i.e. without TiO_2 Anatase) (T) needs to be calculated from the XRD measurements by the proportionality rule, as follow:

$$T = P_{XRD,Anatase}\ x\ \frac{100 - P_{m,Anatase}}{P_{m,Anatase}} \quad (2)$$

With $P_{XRD,\ Anatase}$ is the weight percentage of TiO_2 Anatase measured by the XRD in the total sample.

$P_{m,\ Anatase}$ is the measured weight percentage of TiO_2 Anatase (standard) used in the total sample, which was 10 wt.%.

Then, the real weight percentage of each phase i in the pure sample (i.e. without TiO_2 Anatase) (p_i) was calculated as follow:

$$p_i = \frac{P_{XRD,i}}{T}\ x\ 100 \quad (3)$$

With $P_{XRD,\ i}$ is the weight percentage of phase i measured by XRD in the total sample (i.e. sample & TiO_2 Anatase).

Then, the amorphous weight percentage (A) was calculated by simple difference:

$$A = 100 - \sum p_i \quad (4)$$

Each quantification was performed twice. The average relative error corresponding to the Rietveld analysis was around 5%. Since, the P-XRD analysis was conducted on ash samples,

the results calculated by the mixing rule in the following Figures of the 50-50 wt.% bark-straw biomass mixture will always correspond to 61-39 wt.% bark-straw ash mixture.

2.3.2. SEM-EDX analysis

The tendency to form an amorphous phase together with an analysis of the inorganic semi-quantitative composition of specific samples was evaluated using a Philips XL30 scanning electron microscopy (SEM) equipped with an energy dispersive X-ray fluorescence Oxford Instruments EDX system (INCA software). For the latter, both surface mapping and point analyses were used. Ash test samples of MP2b at 1200°C for 20min and 6h were embedded under vacuum in epoxy resin then were polished with water-free lubricants. A graphite coating was applied to each sample to increase its conductivity, before the analysis.

2.3.3. Sieving measurements

Particles sieving was performed in the ashes collected after the pellet test and the pilot tests. For the pellet test the particle size was measured after putting the ashes in a box, which was shaken for about 1 min to break the loose bridges between particles characterizing their tendency to agglomerate as they could have been done in a pilot test, a method inspired by Steenari et al. [38]. Particle sizes were chosen in the following decreasing order: 4500 µm, 2500 µm, 900 µm, and 630 µm. The particles which size was bigger than 900 µm referred to total agglomerates while the ones which size was smaller than 630 µm were in the solid phase. Particles which size was bigger than 2500 µm were considered as significant agglomerates. The mass fraction in between these meshes was considered to be partially sintered.

For the pilot test, the ashes were collected sieved with the same mesh than for the pellet test, weighed to get the weight percentage, then P-XRD measurements were done for the phases present in each particulate size fraction. Using the weight percentage and the crystalline composition of each fraction, a simple mass balance (mixing rule) was conducted to obtain the average pilot-scale proportion of crystalline and amorphous phases.

3. Results and discussion

3.1. Chemical reaction in comparison with simple mixing effects in the laboratory ash and pellet tests

The P-XRD results on mineralogical compositions after annealing in the ash test (i.e. using compressed ash chips) and after combustion in the pellet test (i.e. using biomass pellets) at 1000℃ for 6h are presented in Figure 1 for pure straw, pure bark, and their 50-50 wt.% biomass mixture (called MP2b). Straw ash in the pellet test melted and interacted within the alumina crucible (Figure A1), so their P-XRD measurements were not possible. In this case, the concentrations of the phases found when pure straw was used in the pellet test were estimated based on the results of pure straw in the pilot fixed bed reactor and in the ash test. Since the P-XRD analysis was conducted on ash samples in both tests, the 50-50 mixing rule in this Figure corresponded to a 61-39 bark-straw ash mixture (β).

The ash of the single fuels reacts at high temperature in combustion reactors [5]. However, the main focus in this work was on the reaction within the ash of the fuel mixtures. The mechanism of reactions are so complex and highly depend on the ash composition and the operating conditions [5,6,28]. Nevertheless, since the ash used in this work were mostly composed of Si, Ca, and K (Table 1), chemical reactions, if taking place, will be governed by the interactions between these three elements in the form of oxides. Si exists in the original biomass in the amorphous SiO_2-H_2O form or in the $Si(OH)_4$ form dissolved in the biomass fluids [5,6]. During combustion or gasification, H_2O will evaporate and SiO_2 will be liberated as small silica particles (SiO_2) due to its higher affinity to oxygen than hydrogen or carbon along with its refractory characteristics [6]. Alkali metals (i.e. K and Na) are the less stable oxides and may be reduced by the carbon-hydrogen fuel matrix to metal vapor in the form of KOH and NaOH [6]. Hence, they can react with the silicates in the matrix following an acid-base reaction to form alkali-silicate oxides [6]. The low eutectic temperatures of the K-Si

252 system, that can be as low as 600℃, makes the formation of agglomerates much easier.
253 Depending on the ash composition of the fuel and in the case of high availability of K in the
254 form of KOH, the density of molten potassium-silicates particles increases significantly. But
255 as the fuel particles are burning out, it shrinks and the ash particles approach each other with
256 an increasing opportunity for contact [6,28]. This will lead to an aggregation of the molten
257 potassium-silicate particles, which will form a larger droplets and initiate slag formation. This
258 explains the abundance of the amorphous phase in the straw samples (Figure 1) since around
259 80 wt.% of the ash of this fuel were composed of Si and K compared to 20 wt.% in bark ash
260 (Table 1). For instance, the results in Figure 1 showed that straw produced ash with high
261 amount of amorphous phase (assumed to be solidified silicate liquid) in both ash and pellet
262 tests at 1000°C (i.e. around 97 wt.%).

263 Fuels, such as woody biomasses, are concentrated with alumina-silicates and calcium-silicates
264 compounds [4]. From Table 1, bark ash contained 71 wt.% calcium compared to 9 wt.% in
265 straw ash. During thermochemical conversion of biomass, the aluminosilicates and calcium-
266 silicates compounds will be probably liberated from the ash matrix as small micrometered-
267 sized particles. This will increase the refractory character of the ash matrix; hence, most of it
268 will remain in the solid form. These compounds are highly stable and have the potentials to
269 increase the melting temperature of the ash [6]. Accordingly, from the results in Figure 1, in
270 the ash test, bark produced ash-rich in solid CaO (47 wt.%) and Ca_2SiO_4 (21 wt.%) along with
271 around just 20 wt.% of amorphous phase. $K_2Ca_6Si_4O_{15}$ was totally absent in the bark ash of
272 the pellet test (it was just 1.8 wt.% in the ash test) with slightly higher concentrations of CaO
273 (53 wt.%) and amorphous phase (22 wt.%) and lower concentration of Ca_2SiO_4 (11 wt.%)
274 than in the ash test. Hence, negligible differences were noticed between the two tests in the
275 case of single biomasses.

276 Chemical reactions within the ash were more apparent when fuels were mixed. The chemical
277 composition of the feedstock was significantly altered upon mixing, which was reflected for
278 example in the change of the calcium over alkali-silicates ratio from 0.1 in the straw and 3.5
279 in the bark to 0.9 in the fuel mixture (Table 1). The low melting point alkali-silicate
280 compounds, can encounter the earth alkali oxide that are mostly concentrated in the bottom
281 ash [6,28,29]. Competition between the earth metals (Ca, Mg) and K on the active sites of the
282 silicate matrix lead to a substitution of K in this matrix by Ca and Mg. This incorporation of
283 earth metals into the agglomerates, due to the high affinity of silicate melts to earth metals [6],
284 increases the melting temperature of the ash and decreases the agglomeration propagation.
285 Several authors showed several reaction pathways for this incorporation leading to more
286 stable compounds that were seen in several studies concerning combustion of biomass, such
287 as $Ca_2K_2Si_9O_{21}$ in the work of Rebling et al. [28] and $K_2Ca_6Si_4O_{15}$ and $K_2Ca_2Si_2O_7$ in the
288 work of Santoso et al. [29].

289 In this work, when straw (rich in alkali-silicate oxides) was mixed with bark (rich in earth
290 alkali oxides), two ternary phases $K_2Ca_6Si_4O_{15}$ (O15) and $K_2Ca_2Si_2O_7$ (O7) appeared in the
291 measured mixture in the ash test. They were not present in the single biomass trials. In
292 parallel, in the ash test, in contrast with the mixing law results (i.e. mixing without chemical
293 interaction), CaO and $CaSiO_3$ were absent in the measured XRD results of the mixture (Figure
294 1). Furthermore, the proportion of the existing phases in the single biomass combustion trials,
295 such as Ca_2SiO_4 (in bark) and K_2SO_4 (in straw), slightly decreased in the mixture, and
296 therefore did not follow the mixing rule. Most importantly, the proportion of the amorphous
297 phase in the ash test, when following the mixing rule without chemical reaction, should be
298 theoretically 50 wt.% in the mixture. However, its contents was measured by the P-XRD to be
299 25 wt.% (Figure 1). Consequently, the presence of chemical reactions within the ash of the
300 biomass mixture in the ash test was confirmed and was dominant over the mixing rule effects.

301 The reactions affected the ash behavior of the biomass mixture by decreasing the amorphous
302 contents beyond the amount predicted by the mixing rule. Hence, biomass mixing can indeed
303 affect the ash behavior through various reactions, which need to be effectively mastered and
304 predicted.

305 Lower proportions of O7 and O15 were found in the pellet test than in the ash test
306 measurements, similar to the results of Defoort et al. [27]. This was the direct consequence of
307 the higher reactivity in the ash test than in the pellet test. Using compressed ash chips, the ash
308 test provided higher physical proximity between inorganic constituents, which was thought to
309 enhance the reactions. Potassium might have reacted with calcium on the silicate matrix instead
310 of volatilizing, to form the new ternary solid phases instead of the amorphous phase [6]. On the
311 contrary, the reaction in the pellet test was less marked due to the presence of organic materials,
312 which evaporated during combustion and left a higher porosity in the sample (i.e. lower grain
313 proximity).

314 Unreacted $CaO/Ca(OH)_2$ is considered as the main crystal product in single bark ash (Figure 1)
315 and as a direct reactant in $K_2Ca_6Si_4O_{15}$ formation. Hence, its presence in mixture samples'
316 reflects a low reactivity level between the inorganic particles in the mixtures. It was observed
317 that $CaO/Ca(OH)_2$ did not transform in the pellet test in the mixture as was the case in the ash
318 test. This means that the bark ash did not fully react with the straw ash when the pellet test was
319 used instead of the ash test. Furthermore, the proportion of the amorphous phase in the pellet
320 test mixture case was close to the one predicted by the mixing rule i.e. without reaction effect
321 between the two biomasses (71 wt.% measured by P-XRD vs 50 wt.% calculated by the mixing
322 rule). Measured Ca_2SiO_4 and $CaO/Ca(OH)_2$ in the pellet test were also successfully predicted
323 by the mixing rule. Hence, contrary to the ash test and despite the presence of chemical
324 reactions, mixing rule effects were dominant in the pellet test.

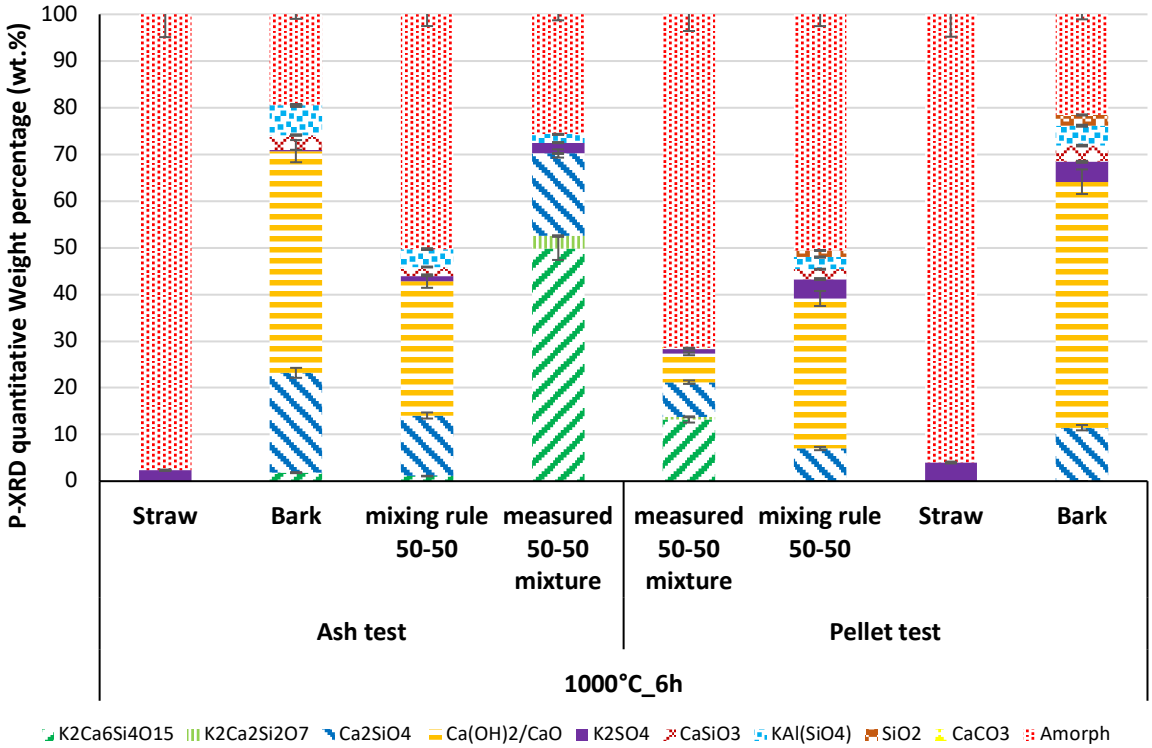

325

326 *Figure 1: P-XRD analysis of single oak bark, single wheat straw, and their mixture at 1000°C after 6h in the*
327 *laboratory ash and pellet tests.*

328 ## 3.2. Effect of operating conditions on ash reactivity

329 The variation of the crystalline and amorphous proportions in MP2b as a function of residence
330 time and temperature are shown in Figures 2 and 4 for the ash and the pellet tests, respectively.
331 For the ash test, long residence times were selected to check if there was a stabilization of the
332 mineralogical composition, i.e. to check if equilibrium was reached (no mass transfer versus
333 time). For the pellet test, no equilibrium was expected due to the significantly lower reactivity
334 between the loose ash particles, as already discussed in section 3.1. Hence, temperature and
335 short residence time close to the ones encountered in the pilot-scale reactors were studied in the
336 pellet test. The impact of the observed cooling rates on the final mineralogical compositions
337 between slow (~0.05 °C/s) and fast (~5 °C/s) cooling in ash test was negligible. Defoort et al.
338 [27] showed in their work that the pelletizing parameters (pellet compression rate) also did not
339 have any effect on the ash reactivity.

3.2.1. Ash test results

In the ash test, the proportion of $K_2Ca_2Si_2O_7$ (light green) increased 4 wt.% at 850°C while it decreased from 13 wt.% to 1 wt.% at 1000°C (Figure 2) with the increase in residence time. It should be noted that drawing clear conclusions at 850°C is limited due to the few experimental points (just two experimental conditions for 6h and 24h). However, more experimental points at 1000°C compensated this limitation, and adding the two experimental points at 850°C contributed to the demonstration of the overall ash behavior with respect to temperature and residence time variation. The amount of $K_2Ca_6Si_4O_{15}$ (dark green) exhibited a parabolic behavior that peaked at around 50 wt.% (i.e. equilibrium is reached when mass transfer ceased) at 1000°C and 5h to 6h, conditions that were considered as optimum for this type of mixture. The increase in O15 at the expense of O7 proportions at 1000°C in this work supports the reactant-product reversible reaction pathway between these two crystalline structures, as presented in the work of Santoso et al. [29]. In their work, Santoso et al. suggested the reaction of $K_2Ca_2Si_2O_7$ with calcium-silicate compounds to produce $K_2Ca_6Si_4O_{15}$ [29]. The formation of this phase, either from the aforementioned possible reaction or from the reaction of the calcium earth metals in the bark with the potassium-silicates in the straw, decreased the available amount of silicates that can react with potassium, hence in turn can limit the amorphous phase formation. This was indeed confirmed from the results in Figure 2 where the appearance of $K_2Ca_6Si_4O_{15}$ was always conjugated with a decrease in the amorphous phase. For instance, the increase of O15 from 8 wt.% to 51 wt.% was conjugated with a decrease in the amorphous concentration from 43 wt.% to 26 wt.% as residence time increased from 20 min to 40h at 1000°C. Hence, when using bark-straw biomass mixture in a furnace or a FB, mixture formulation and reactor operation should be directed in a way to obtain the highest proportion possible of $K_2Ca_6Si_4O_{15}$.

Similar amounts of Ca_2SiO_4 were also present in all samples. Minor proportions of $CaO/Ca(OH)_2$ were observed at 850°C and 1000°C at short residence times, but this compound was absent at 1000°C and long residence times (5h) and at 1200°C. This, in turn, supports the finding that reaction was complete and equilibrium was reached for 1000°C at 5h and 1200°C at around 3h.

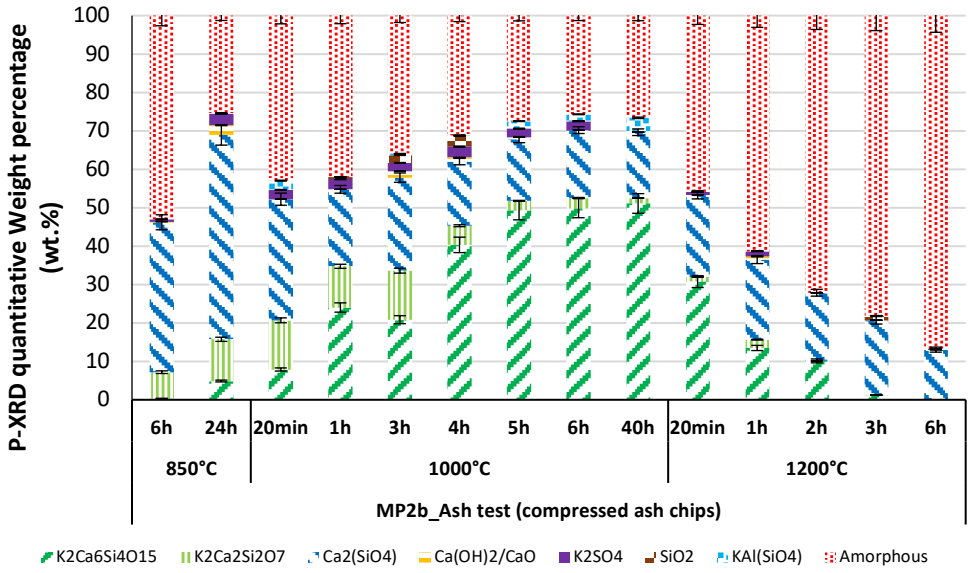

Figure 2: P-XRD results of the ash test at various temperatures and residence times.

As can be seen in Figure 2, with the increase in residence time at 1200°C, equilibrium was approached after around 3h, conditions at which $K_2Ca_6Si_4O_{15}$ and $K_2Ca_2Si_2O_7$ were decomposed. To validate this decomposition, SEM-EDX analysis as presented in Figure 3 showed the variation of the phases at 1200°C between 20min (Figure 3.a) and 6h (Figure 3.b) in the MP2b biomass mixture for each different shape, and the results were also compared to the ones of Chen et al. [39]. Electron probe X-ray microanalysis (EPMA) techniques were used in their work starting from various mixtures of $CaCO_3$-K_2CO_3-SiO_2 [39]. They provided EPMA pictures for the crystalline phases of interest [39].

Following the results in Figure 2, the ternary phases of interest, $K_2Ca_6Si_4O_{15}$ and $K_2Ca_2Si_2O_7$, were present at 20min in Figure 3.a but absent at 6h in Figure 3.b at 1200°C. According to the EDX analysis and similarly to the findings of Chen et al. [39], $K_2Ca_6Si_4O_{15}$ has a rectangular-

oval shape while $K_2Ca_2Si_2O_7$ looks like long sticks and Ca_2SiO_4 was characterized by a circular shape.

For the case of 20 min residence time (Figure 3.a), the sample was highly heterogeneous, while the one at 6h was characterized by its higher homogeneous propensity. The equilibrium, supported by the P-XRD results in Figure 2, might have affected this varying morphology transforming a heterogeneous structure into a more homogenous one as it was reached. $K_2Ca_6Si_4O_{15}$ in the 20 minutes sample (Figure 3.a) was highly surrounded by amorphous layers, which refers to its possible disappearance at 1200°C with increasing time (i.e. as equilibrium was approached) by fusion and reaction with elements in the liquid phase.

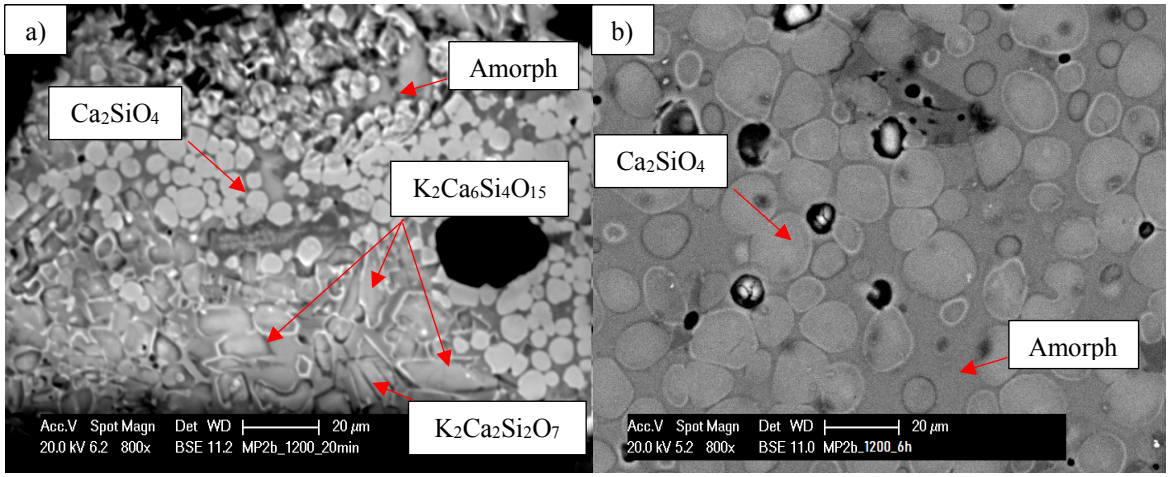

Figure 3: SEM-EDX analysis between 20min (a) and 6h (b) for MP2b at 1200°C in ash test.

3.2.2. Pellet test results

Figure 4 shows the P-XRD results of the pellet test using the 50-50 blend under various operating conditions. The two ternary compounds $K_2Ca_6Si_4O_{15}$ and $K_2Ca_2Si_2O_7$ in the pellet test, as visible in Figure 4, showed similar behavior to those in the ash test with respect to temperature (at 850°C and 1000°C) and residence times, but with significantly lower proportions than the ash test. This was due to the lower reactivity in the pellet test, as explained in section 3.1, under the same operating conditions. This lower reactivity was also visible in the negligible change in the amorphous phase proportion and its constant high proportion along

with the constant presence of CaO under all operating conditions. Hence, due to this lower reactivity level and in contrast with the ash test, the effects of operating conditions on ash reactivity of biomass mixtures in the pellet test were less significant.

Though by comparing the composition of the samples between 850°C and 1000°C at the same residence time (20min then 1h), the mineralogical compositions changed, which can be attributed to an increased reactivity with temperature since $CaCO_3$ present at 850°C was calcined to CaO at 1000°C and 20 min then reacted. Four-time less CaO was found at 1000°C after 1h while four-time more $K_2Ca_6Si_4O_{15}$ was found due to chemical reaction, but both with low overall concentrations. Authors of this work doubt that the pellet test will ever reach a complete equilibrium state since the distance between the inorganic particles will never be close enough to each other and due to the presence of the organic matrix in the samples, contrary to the case of the ash test.

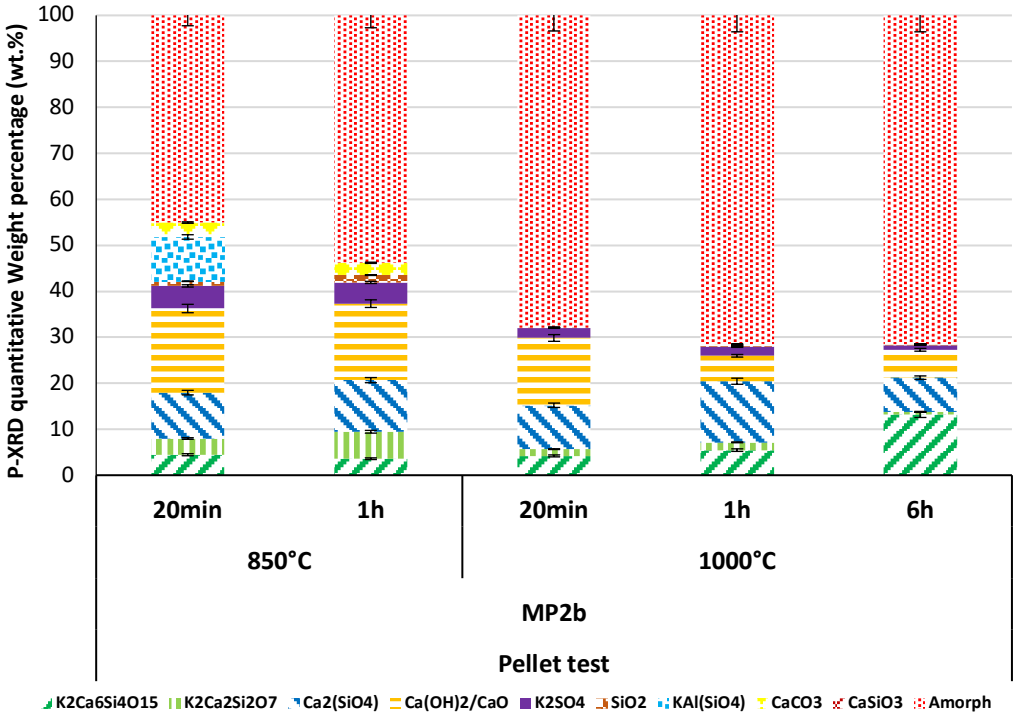

Figure 4: P-XRD results of the pellet test at various temperatures and residence times in the 50-50 blend (MP2b).

Figure 5 shows the sieving fractions of the produced ash from the MP2b mixture under the various operating conditions. Particles smaller than 630µm refer to solid powder whereas those bigger than 900µm are considered as being agglomerates. Agglomerates are considered to be formed of big pieces of amorphous phases entrapping minor amounts of crystalline compounds. Hence, the concentrations of the amorphous phase and the ones of agglomerates are directly correlated and proportional.

It can be seen from the results in Figure 5 that in the pellet test for the case of the 50-50 biomass mixture, the fraction of the large particle size (agglomerates > 900µm) increased with the increase in residence time. It can also be seen that temperature affected the formation of agglomerates by comparing the pellet test between 850°C and 1000°C under a fixed residence time of 1h, where large particle size fraction significantly increased from 38 wt.% to 57 wt.%.

In Figure 5, agglomerates' weight fractions above 900µm at 1000°C were 60 wt.% at 20min, 55 wt.% at 1h, and 83 wt.% at 6h. In comparison, from Figure 4, the amorphous phase fraction quantified by P-XRD for the pellet test under the same operating conditions were 68 wt.%, 71 wt.%, and 71 wt.%, respectively. Hence, the percentage of errors between the two methodologies were 13%, 29% and 14%, respectively, meaning an error of 18.67% on average. Taking into account the small sample weights used in the sieving of the pellet test that can induce several measurement errors and the fact that agglomerates entrap a certain amount of crystalline phases, it can be said that both methods can be to a certain extent used for amorphous quantification, with an emphasize on the PXRD-internal standard-Rietveld refinement methodology.

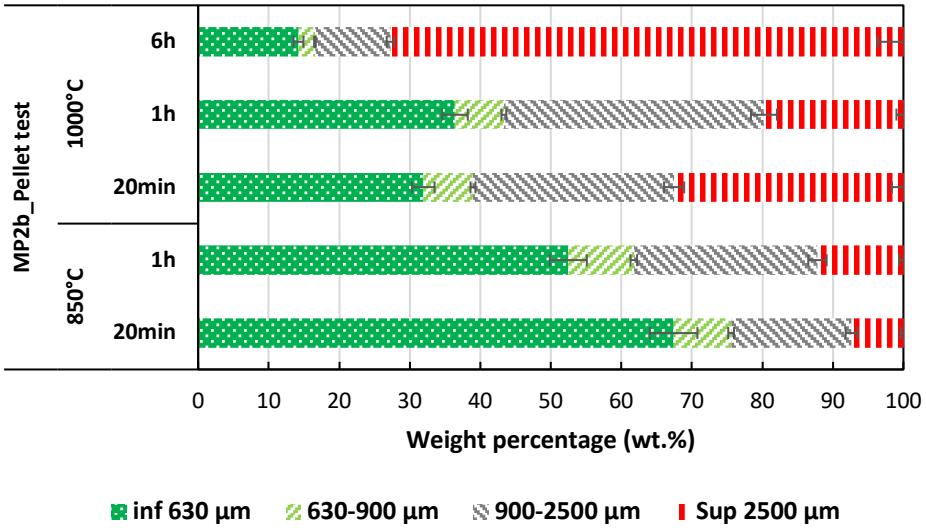

Figure 5: Particles size distribution of ash pellet test using MP2b under various operating conditions.

3.3. Laboratory test results comparison with pilots

Figure 6 shows the P-XRD results of the ashes collected after the pellet combustion of single biomass (bark, straw) and 50-50 bark-straw mixture in the fixed and moving bed combustion pilots. Moreover this figure shows the results of the mixing rule calculated from the ashes collected from the fixed bed pilot test using each single feedstock.

Temperature measurements results along with gaseous emissions (i.e. CO and NO_x) were shown in the Appendix, but are out of scope in this work. In the moving grid pilot reactor, the temperature was estimated to be in the range of 900°C ± 20°C and the residence time around 20 min ± 3 min. In the fixed bed reactor, residence time was around 2h, and the combustion temperature was measured and was found to be 700°C when wheat straw was applied, 950°C when the bark was used, and around 1000°C in the case of the blend. 78 wt.% of the ash of wheat straw was composed of Si and K while 71 wt.% of bark ash was made of Ca (Table 1). As explained in section 3.1, the high alkali contents will react with the silica matrix and significantly lower the ash melting point [6]. On the other hand, the high calcium contents will stabilize the melting behavior of the ash and increase its melting point [6]. For instance, wheat straw is known to melt between 400°C and 960°C, reaching severe melting at

454 temperatures between 680°C and 780°C [35] while bark is more stable even at a high
455 temperature of 1000°C (melting 1060°C-1500°C [23,35]). This was in total accord with the
456 combustion temperatures for straw and bark found in this work. The presence of melts will
457 cause sintering and corrosion inside the burning chamber and hence push the gaseous
458 proportion outside their acceptable toxic range [22,33]. When bark was mixed with straw, Ca
459 contents increased to 42wt.% compared to straw, and hence along with the chemical
460 interaction between the inorganic compounds coming from the fuel mixing that created stable
461 ternary phases, increased the combustion temperature of the mixture.

462 It is observed, in Figure 6, that in the fixed bed pilot, straw was rich in amorphous contents (95
463 wt.%) while the bark was more abundant with CaO (31 wt.%) and Ca_2SiO_4 (21 wt.%).
464 $K_2Ca_2SiO_7$ (first ternary phase) and $K_2Ca_6Si_4O_{15}$ (second ternary phase) were absent or
465 negligible in the ash of the single straw and single bark on pilot level. However, $K_2Ca_2SiO_7$ and
466 $K_2Ca_6Si_4O_{15}$ were both identified in the samples of the biomass mixture after experiments in
467 both pilot reactors. CaO calculated to be at 22 wt.% by the mixing rule in the blend was
468 measured at around 5 wt.% in the fixed bed reactor and 7 wt.% in the moving grid reactor.
469 Ca_2SiO_4 and amorphous contents were predicted to be 15 wt.% and 52 wt.% by the mixing rule
470 calculation. In comparison, they were measured at 19 wt.% and 60 wt.% in the fixed bed reactor
471 and 10 wt.% and 69 wt.% in the moving grid pilot reactor. Hence, similarly to the laboratory
472 pellet test experiments, despite the abundance of the mixing effect without interaction, a
473 reaction within the ash took place in both pilot reactors.

474 Both pilots used the same biomass pellets of the laboratory pellet test. Hence, the pellet test,
475 specifically at 1000°C for 20 minutes and 1h can be used to possibly simulate/predict the pilot-
476 scale ash behavior. Pellet test P-XRD results of MP2b at 1000°C and 1h in Figure 4 were close
477 to the ones measured on pilot scale, recording 71 wt.% amorphous phase, 5 wt.% $K_2Ca_6Si_4O_{15}$,
478 5 wt.% CaO and 13 wt.% Ca_2SiO_4. Similarly, close phase distributions were exhibited in the

479 case of single biomasses by comparing the results in Figures 1 and 6. Consequently, despite the
480 scale increase between the pellet test and the pilots, the pellet test showed great prediction
481 capabilities for the pilots in terms of crystalline and amorphous phases' fractions for both single
482 feedstock and their biomass mixture.

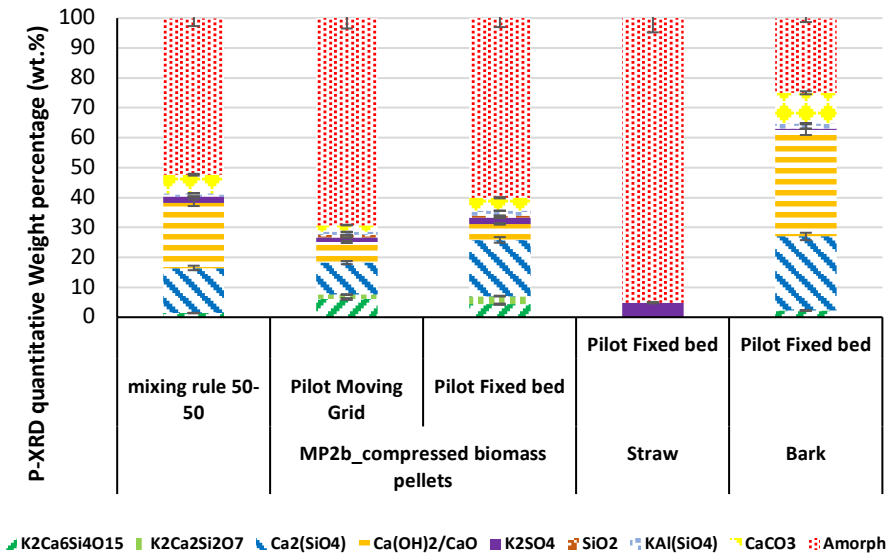

483
484 *Figure 6: P-XRD average crystalline and amorphous distribution in pilot reactors.*

485 The sieving fractions of the produced ash from the fixed and moving bed reactors were plotted
486 for the single bark, single straw, and MP2b mixture in Figure 7. Furthermore the mixing rule
487 was also calculated from the ashes of the single biomass of the fixed bed reactor and plotted on
488 the same Figure.

489 Particles smaller than 630µm referred to solid powder whereas those bigger than 900µm are
490 considered as being agglomerates. Straw was problematic if applied in a furnace since more
491 than 75 wt.% of it showed significant agglomeration (>2500µm) and around 84 wt.% total
492 agglomeration (>900µm). Bark was ideal for furnace combustion application since more than
493 60 wt.% of it remained as a solid powder (<630µm). Without chemical reaction (i.e. mixing
494 rule is valid), significant agglomeration should theoretically be in the range of 47 wt.%
495 (>2500µm) and total agglomeration around 60 wt.% (>900µm). However, the presence of

chemical reactions within the ash of the feedstock mixture further enhanced the decrease of the significant agglomeration to less than 25 wt.%, (>2500µm) and total agglomeration to around 50 wt.% (>900µm), on average. This made the application of straw in the pilot boiler less problematic when mixed with bark.

It should be noted that the mass of agglomerate fractions above 900µm of bark, straw, and the biomass mixture of both pilot reactors in Figure 7 were close and proportional to the amorphous phase fraction quantified by PXRD in Figure 6 (95 wt.% in Figure 6 VS 84 wt.% in Figure 7 for straw, 25 wt.% in Figure 6 VS 37 wt.% in Figure 7 for bark, 65 wt.% in Figure 6 VS 53 wt.% in Figure 7 for the mixtures on average). Hence, both methods can provide amorphous / agglomeration quantification. In parallel, from the sieving fractions of the pellet test at 1000°C and 1h for the mixture case in Figure 5, total agglomeration was measured to be 57 wt.% while the one of pilots in Figure 7 was measured to be 53 wt.% on average. Hence, the pellet test was also able to predict the agglomerates proportion of the pilot reactors.

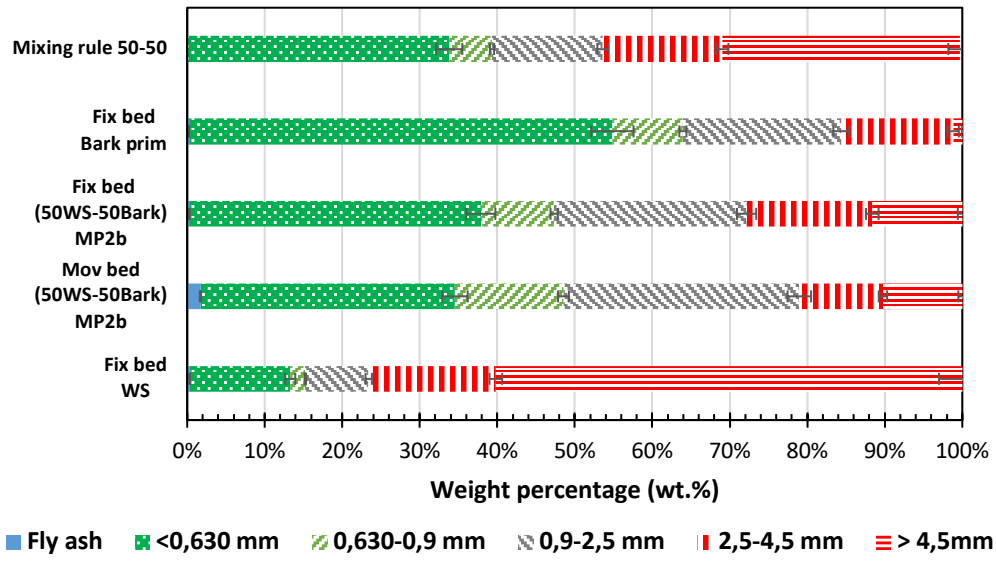

Figure 7: Particles size distribution of ash in the pilots' reactors using single bark, single straw, and MP2b mixture.

4. Conclusion

Chemical reactions effect was dominant when ash mixtures (i.e. ash test) were used while mixing rule influence was the most important when biomass mixtures were applied on both laboratory (i.e. pellet test) and pilot scales, with only a small chemical reactivity found in the second case. Hence, in terms of tests, ash reactivity can be ranked in the decreasing order as follow: ash test > pellet test > pilot. This in turn affected the effects of operating conditions on ash behavior that were ranked in the same aforementioned order.

The temperature then residence time had higher effects on ash reactivity than cooling and pellet compression rates. $K_2Ca_6Si_4O_{15}$ and $K_2Ca_2Si_2O_7$ were the main products of the chemical reactions in 50-50 bark-straw biomass and ash mixtures. They were absent in the single feedstock but highly stable at 1000°C and 6h in the blend in the ash test, conditions at which equilibrium was experimentally reached. Their appearance along with their increasing proportions led to a decrease in the amorphous proportion. Hence, optimizing the blend to increase their concentration has the potential to solve slagging problematic.

Laboratory pellet test was able to predict pilot behavior in terms of crystalline and amorphous proportions along with agglomeration distribution for both individual biomasses and biomass mixtures. Hence, using the pellet laboratory test before any pilot operation has the potential to make economic savings and reduce operational problems related to ash behavior in pilot and industrial scale reactors. These results should be checked for other biomass mixtures as well as in the case of FBR where biomass ash may also react with the bed materials.

References

[1] Bhaskar T, Pandey A. Advances in Thermochemical Conversion of Biomass—Introduction. Recent Adv. Thermo-Chem. Convers. Biomass, Elsevier; 2015, p. 3–30. https://doi.org/10.1016/B978-0-444-63289-0.00001-6.

[2] Scarlat N, Dallemand J-F, Monforti-Ferrario F, Nita V. The role of biomass and bioenergy in a future bioeconomy: Policies and facts. Environ Dev 2015;15:3–34. https://doi.org/10.1016/j.envdev.2015.03.006.

[3] Vassilev SV, Vassileva CG, Song Y-C, Li W-Y, Feng J. Ash contents and ash-forming elements of biomass and their significance for solid biofuel combustion. Fuel 2017;208:377–409. https://doi.org/10.1016/j.fuel.2017.07.036.

[4] Vassilev SV, Baxter D, Andersen LK, Vassileva CG. An overview of the chemical composition of biomass. Fuel 2010;89:913–33. https://doi.org/10.1016/j.fuel.2009.10.022.

[5] Vassilev SV, Baxter D, Vassileva CG. An overview of the behaviour of biomass during combustion: Part I. Phase-mineral transformations of organic and inorganic matter. Fuel 2013;112:391–449. https://doi.org/10.1016/j.fuel.2013.05.043.

[6] Boström D, Skoglund N, Grimm A, Boman C, Öhman M, Broström M, et al. Ash Transformation Chemistry during Combustion of Biomass. Energy Fuels 2012;26:85–93. https://doi.org/10.1021/ef201205b.

[7] Öhman M, Nordin A, Skrifvars B-J, Backman R, Hupa M. Bed Agglomeration Characteristics during Fluidized Bed Combustion of Biomass Fuels. Energy Fuels 2000;14:169–78. https://doi.org/10.1021/ef990107b.

[8] Ma C, Weiland F, Hedman H, Boström D, Backman R, Öhman M. Characterization of Reactor Ash Deposits from Pilot-Scale Pressurized Entrained-Flow Gasification of Woody Biomass. Energy Fuels 2013;27:6801–14. https://doi.org/10.1021/ef401591a.

[9] Froment K, Seiler JM, Poirier J, Colombel L. Determining Cooling Screen Slagging Reactor Operating Temperature. Energy Fuels 2015;29:5069–77. https://doi.org/10.1021/acs.energyfuels.5b00744.

[10] Mack R, Kuptz D, Schön C, Hartmann H. Combustion behavior and slagging tendencies of kaolin additivated agricultural pellets and of wood-straw pellet blends in a small-scale boiler. Biomass Bioenergy 2019;125:50–62. https://doi.org/10.1016/j.biombioe.2019.04.003.

[11] Holubcik M, Jandacka J, Palacka M, Vician P. Additives application to wheat straw to increasing the ash fusion temperature. AIP Conf Proc 2016;1768:020014. https://doi.org/10.1063/1.4963036.

[12] Wang C, Zhao L, Sun R, Hu Y, Tang G, Chen W, et al. Effects of silicon-aluminum additives on ash mineralogy, morphology, and transformation of sodium, calcium, and iron during oxy-fuel combustion of zhundong high-alkali coal. Int J Greenh Gas Control 2019;91:102832. https://doi.org/10.1016/j.ijggc.2019.102832.

[13] Yao X, Zhou H, Xu K, Xu Q, Li L. Evaluation of the fusion and agglomeration properties of ashes from combustion of biomass, coal and their mixtures and the effects of K2CO3 additives. Fuel 2019;255:115829. https://doi.org/10.1016/j.fuel.2019.115829.

[14] Wang L, Hustad JE, Skreiberg Ø, Skjevrak G, Grønli M. A Critical Review on Additives to Reduce Ash Related Operation Problems in Biomass Combustion Applications. Energy Procedia 2012;20:20–9. https://doi.org/10.1016/j.egypro.2012.03.004.

[15] Míguez JL, Porteiro J, Behrendt F, Blanco D, Patiño D, Dieguez-Alonso A. Review of the use of additives to mitigate operational problems associated with the combustion of biomass with high content in ash-forming species. Renew Sustain Energy Rev 2021;141:110502. https://doi.org/10.1016/j.rser.2020.110502.

584 [16] Nguyen HK, Moon JH, Jo SH, Park SJ, Bae DH, Seo MW, et al. Ash characteristics of
585 oxy-biomass combustion in a circulating fluidized bed with kaolin addition. Energy
586 2021;230:120871. https://doi.org/10.1016/j.energy.2021.120871.
587 [17] Zhou C, Rosén C, Engvall K. Biomass oxygen/steam gasification in a pressurized
588 bubbling fluidized bed: Agglomeration behavior. Appl Energy 2016;172:230–50.
589 https://doi.org/10.1016/j.apenergy.2016.03.106.
590 [18] Wang Q, Han K, Wang P, Li S, Zhang M. Influence of additive on ash and combustion
591 characteristics during biomass combustion under O2/CO2 atmosphere. Energy
592 2020;195:116987. https://doi.org/10.1016/j.energy.2020.116987.
593 [19] Fournel S, Palacios JH, Godbout S, Heitz M. Effect of Additives and Fuel Blending on
594 Emissions and Ash-Related Problems from Small-Scale Combustion of Reed Canary
595 Grass. Agriculture 2015;5:561–76. https://doi.org/10.3390/agriculture5030561.
596 [20] Thy P, Jenkins BM, Williams RB, Lesher CE, Bakker RR. Bed agglomeration in
597 fluidized combustor fueled by wood and rice straw blends. Fuel Process Technol
598 2010;91:1464–85. https://doi.org/10.1016/j.fuproc.2010.05.024.
599 [21] Zeng T, Pollex A, Weller N, Lenz V, Nelles M. Blended biomass pellets as fuel for
600 small scale combustion appliances: Effect of blending on slag formation in the bottom
601 ash and pre-evaluation options. Fuel 2018;212:108–16.
602 https://doi.org/10.1016/j.fuel.2017.10.036.
603 [22] Zeng T, Weller N, Pollex A, Lenz V. Blended biomass pellets as fuel for small scale
604 combustion appliances: Influence on gaseous and total particulate matter emissions and
605 applicability of fuel indices. Fuel 2016;184:689–700.
606 https://doi.org/10.1016/j.fuel.2016.07.047.
607 [23] Thy P, Jenkins BM, Lesher CE, Grundvig S. Compositional constraints on slag
608 formation and potassium volatilization from rice straw blended wood fuel. Fuel Process
609 Technol 2006;87:383–408. https://doi.org/10.1016/j.fuproc.2005.08.015.
610 [24] Rodríguez JL, Álvarez X, Valero E, Ortiz L, Torre-Rodríguez N de la, Acuña-Alonso C.
611 Design of solid biofuels blends to minimize the risk of sintering in biomass boilers. J
612 Energy Inst 2020;93:2409–14. https://doi.org/10.1016/j.joei.2020.07.015.
613 [25] Royo J, Canalís P, Quintana D, Díaz-Ramírez M, Sin A, Rezeau A. Experimental study
614 on the ash behaviour in combustion of pelletized residual agricultural biomass. Fuel
615 2019;239:991–1000. https://doi.org/10.1016/j.fuel.2018.11.054.
616 [26] Skrifvars B-J, Öhman M, Nordin A, Hupa M. Predicting bed agglomeration tendencies
617 for biomass fuels fired in FBC boilers: A comparison of three different prediction
618 methods. Energy Fuels 1999;13:359–63. https://doi.org/10.1021/ef980045+.
619 [27] Defoort F, Campargue M, Ratel G, Miller H, Dupont C. Physicochemical Approach To
620 Blend Biomass. Energy Fuels 2019;33:5820–8.
621 https://doi.org/10.1021/acs.energyfuels.8b04169.
622 [28] Rebbling A, Sundberg P, Fagerström J, Carlborg M, Tullin C, Boström D, et al.
623 Demonstrating Fuel Design To Reduce Particulate Emissions and Control Slagging in
624 Industrial-Scale Grate Combustion of Woody Biomass. Energy Fuels 2020;34:2574–83.
625 https://doi.org/10.1021/acs.energyfuels.9b03935.
626 [29] Santoso I, Taskinen P, Jokilaakso A, Paek M-K, Lindberg D. Phase equilibria and liquid
627 phase behavior of the K2O-CaO-SiO2 system for entrained flow biomass gasification.
628 Fuel 2020;265:116894. https://doi.org/10.1016/j.fuel.2019.116894.
629 [30] Salour D, Jenkins BM, Vafaei M, Kayhanian M. Control of in-bed agglomeration by fuel
630 blending in a pilot scale straw and wood fueled AFBC. Biomass Bioenergy 1993;4:117–
631 33. https://doi.org/10.1016/0961-9534(93)90033-Z.

[31] Nordgren D, Hedman H, Padban N, Boström D, Öhman M. Ash transformations in pulverised fuel co-combustion of straw and woody biomass. Fuel Process Technol 2013;105:52–8. https://doi.org/10.1016/j.fuproc.2011.05.027.
[32] Wang L, Skreiberg Ø, Becidan M. Investigation of additives for preventing ash fouling and sintering during barley straw combustion. Appl Therm Eng 2014;70:1262–9. https://doi.org/10.1016/j.applthermaleng.2014.05.075.
[33] Regueiro A, Patiño D, Granada E, Porteiro J. Experimental study on the fouling behaviour of an underfeed fixed-bed biomass combustor. Appl Therm Eng 2017;112:523–33. https://doi.org/10.1016/j.applthermaleng.2016.10.105.
[34] Royo J, Canalís P, Quintana D. Chemical study of fly ash deposition in combustion of pelletized residual agricultural biomass. Fuel 2020;268:117228. https://doi.org/10.1016/j.fuel.2020.117228.
[35] Link S, Yrjas P, Hupa L. Ash melting behaviour of wheat straw blends with wood and reed. Renew Energy 2018;124:11–20. https://doi.org/10.1016/j.renene.2017.09.050.
[36] Vega-Nieva D, Alvarez C, Ortiz L. Results of new laboratory methods and slagging classification systems for the prediction and quantification of ash slagging in woody and herbaceous biomass fuels. Cent. Eur. Biomass Conf., 2014.
[37] Gilbe C, Lindström E, Backman R, Samuelsson R, Burvall J, Öhman M. Predicting Slagging Tendencies for Biomass Pellets Fired in Residential Appliances: A Comparison of Different Prediction Methods. Energy Fuels 2008;22:3680–6. https://doi.org/10.1021/ef800321h.
[38] Steenari B-M, Lundberg A, Pettersson H, Wilewska-Bien M, Andersson D. Investigation of ash sintering during combustion of agricultural residues and the effect of additives. Energy Fuels 2009;23:5655–62. https://doi.org/10.1021/ef900471u.
[39] Chen M, Hou X, Chen J, Zhao B. Phase Equilibria Studies in the SiO2-K2O-CaO System. Metall Mater Trans B 2016;47:1690–6. https://doi.org/10.1007/s11663-016-0623-z.